

F. Porcelli, G. Bateman, L.-G. Eriksson, D. Grasso, J. Graves, T. Hellsten, G. Huysmans,  
T. Johnson, A. Kritz, H. Lütjens, M.-L. Mayoral, M.F. Nave, C.N. Nguyen, A. Pankin,  
A. Perona, S.D. Pinches, P. Sandquist, O. Sauter, S. Sharapov, I. Voitsekhovich,  
F. Zonca the European Task Force on Integrated Modelling Activity  
and JET EFDA contributors

# Integrated Modelling of Sawtooth Oscillations in Tokamak Plasmas

"This document is intended for publication in the open literature. It is made available on the understanding that it may not be further circulated and extracts or references may not be published prior to publication of the original when applicable, or without the consent of the Publications Officer, EFDA, Culham Science Centre, Abingdon, Oxon, OX14 3DB, UK."

"Enquiries about Copyright and reproduction should be addressed to the Publications Officer, EFDA, Culham Science Centre, Abingdon, Oxon, OX14 3DB, UK."

# Integrated Modelling of Sawtooth Oscillations in Tokamak Plasmas

F. Porcelli<sup>1</sup>, G. Bateman<sup>2</sup>, L.-G. Eriksson<sup>3</sup>, D. Grasso<sup>1</sup>, J. Graves<sup>4</sup>, T. Hellsten<sup>5</sup>,  
G. Huysmans<sup>3</sup>, T. Johnson<sup>5</sup>, A. Kritz<sup>2</sup>, H. Lütjens<sup>6</sup>, M.-L. Mayoral<sup>7</sup>, M.F. Nave<sup>8</sup>,  
C.N. Nguyen<sup>2</sup>, A. Pankin<sup>9</sup>, A. Perona<sup>1</sup>, S.D. Pinches<sup>7</sup>, P. Sandquist<sup>10</sup>, O. Sauter<sup>4</sup>,  
S. Sharapov<sup>7</sup>, I. Voitsekhovich<sup>8</sup>, F. Zonca<sup>11</sup> the European Task Force on  
Integrated Modelling Activity<sup>12</sup> and JET EFDA contributors\*

<sup>1</sup>Burning Plasma Research Group, Department of Energetics, Politecnico di Torino, Italy

<sup>2</sup>Lehigh University Physics Department, Bethlehem, PA 18015, USA

<sup>3</sup>Association EURATOM-CEA, CEA/DSM/DRFC, CEA-Cadarache, France

<sup>4</sup>CRPP, Association EURATOM-Confederation Suisse, EPFL, 1015 Lausanne, Switzerland

<sup>5</sup>Alfvén Laboratory, Association VR-Euratom, Stockholm, Sweden

<sup>6</sup>CPHT Ecole Polytechnique, UMR-7644 du CNRS, Palaiseau, France

<sup>7</sup>Euratom/UKAEA Fusion Association, Culham Science Centre, Abingdon OX14 3DB, UK

<sup>8</sup>Euratom/IST Fusion Association, Centro de Fusao Nuclear, Lisboa, Portugal

<sup>9</sup>SAIC, San Diego, CA 92121, USA

<sup>10</sup>Euratom/VR Fusion Association, Chalmers Univ. of Technology, Goteborg, Sweden

<sup>11</sup>Association Euratom/ENEA/CNR Fusione, Frascati, Italy

<sup>12</sup><http://www.efda-taskforce-itm.org>

\* See annex of M. L. Watkins et al, “Overview of JET Results”,  
(Proc. 21<sup>st</sup> IAEA Fusion Energy Conference, Chengdu, China (2006)).



## ABSTRACT.

The paper investigates the evolution of  $\gamma$ -ray emission induced by fusion alphas colliding with beryllium impurity ions in tritium NBI blip experiments on JET. We assess the possible evaluation of slowing down and alpha loss rates from measurements of the delay time between gamma emission and alpha production in DT fusions. Such measurements are then compared with 3D Fokker-Planck modelling. Losses additional to first orbit loss of fusion alphas are validated for low I / low B and Current Hole (CH) plasmas. Finally, we identify the requirements for  $\gamma$ -ray diagnostics as well as for the plasma and the tritium NBI conditions that are optimised to provide information on the confinement of fusion born  $\alpha$ -particles.

## 1. INTRODUCTION

The investigation of fusion born alpha particles, produced in JET by tritium NBI blips into deuterium plasmas, by the use of  $\gamma$ -diagnostics [1-3] is a new and promising approach in the study of fast ion behaviour in tokamak plasmas. In these experiments, the information about charged fusion products in the *MeV* energy range is inferred from measurements of  $\gamma$ -ray emission arising from nuclear interactions of alphas with beryllium impurity ions. One of the most important issues that can be addressed by such  $\gamma$ -ray diagnostics is the possibility of assessing experimentally the confinement properties of fusion born  $\alpha$ -particles in plasmas with new types of magnetic topology, such as the Current Hole (CH) equilibrium observed on JET [4] and JT-60U [5]. In previous modelling reported in Refs. [3, 6-9], it was found that the interpretation of the experimentally observed evolution of  $\alpha$ -produced  $\gamma$ -ray emission requires not only the calculation of  $\alpha$ -particle transport, but also an equally accurate description of the time dependence and the shape of the fusion source determined by the tritium NBI blips and the deuterium plasma. Here we present a detailed modelling of the evolution of  $\alpha$ -particles produced in JET by tritium NBI into a deuterium plasma and identify the best options for future measurements of fast alpha confinement based on  $\gamma$ -ray diagnostics. Particularly, the possibility of evaluating the loss rate of fusion alphas from the delay time between the alpha induced  $\gamma$ -emission and the fusion source is shown to be a viable technique.

## 2. Delay of alpha-induced $\gamma$ -emission: qualitative analysis

In the case of steady-state beryllium ion density at low temperature, the time evolution of the  $\gamma$ -emission rate  $R_\gamma$  is determined as

$$R_\gamma(t) \propto \int dE E F_\alpha(E,t) \sigma_\gamma(E), \quad (1)$$

where  $f_\alpha(E,t)$  denotes the alpha distribution function and  $\sigma_\gamma$  the  $^9\text{Be}(\alpha,n\gamma)^{12}\text{C}$  reaction cross-section. Using the simplest kinetic equation for *MeV*-alphas that takes into account only the energy and time dependences of their distribution and considers their loss in the average loss time ( $\tau_l$ ) - approximation,

$$\partial_t f = 2E^{-1/2} \tau_s - {}^I\partial_E (E^{3/2} f) - f/\tau_l + S(E,t), \quad (2)$$

the RHS of Eq. (1) can be readily expressed as

$$R_\gamma(t) \propto \int_{E_m}^{\infty} dE \sqrt{E} \int_0^{\tau_{\alpha\gamma}} d\tau \sigma_\gamma(E') \sqrt{E'} \exp\left(-\frac{\tau}{\tau_l}\right) S(E, t-\tau), \quad (3)$$

where

$$\partial_t f = 2E^{-1/2} \tau_s - {}^1\partial_E (E^{3/2} f) - f/\tau_l + S(E, t), \quad (4)$$

$\tau_s \sim T_e^{3/2}/n$  is the Spitzer slowing down time,  $S$  the alpha source term and  $\tau_{\alpha\gamma}$  is the slowing down time of alphas from their birth energy to  $E_m \approx 1.6$  MeV representing the threshold energy for the  $\gamma$ -emission reaction  ${}^9\text{Be}(\alpha, n\gamma){}^{12}\text{C}$ . In the simplest case of a monoenergetic alpha source that is effective only in a short time interval at  $t=0$ , i.e.  $S \sim \delta(E - E_0, t)$ , the time behaviour of gamma emission is completely determined by the energy dependence of the cross section  $\sigma_\gamma$  and the alpha confinement

$$R_\gamma(t) \propto \exp\left(-\frac{t}{\tau_l}\right) \sigma_\gamma(E) \sqrt{E}, \quad E = E_0 \exp\left(-\frac{t}{\tau_l}\right) \quad (5)$$

Figure 1 demonstrates the evolution of gamma emission produced by a  $\delta(E-E_0, t)$ -source with  $E_0 = 3.5$  MeV. In the case of well confined alphas the maximum  $\gamma$ -ray emission is seen to be induced by alphas slowed down to energies  $E \sim 1.8 \div 2$  MeV and to appear delayed against the alpha production by about 30% of the Spitzer slowing down time. Taking an average loss time  $\tau_l = \tau_s/3$ , the alpha loss will reduce both the gamma emission as well as its delay. As a quantitative characteristic of gamma delay,  $\tau_d$ , we use here the position of the “centroid” of  $R_\gamma(t)$  determining the moment when the gamma yield  $I(t) = \int dt R_\gamma(t)$  is half of its total, i.e.  $I(\tau_d) = 0.5I(\tau_{\alpha\gamma})$ . Gamma emission induced by well confined alphas is delayed by about  $0.24\tau_s$  ( $\sim 0.6\tau_{\alpha\gamma}$ ). Degradation of the alpha confinement corresponding to a loss time  $\tau_l = \tau_s/3$  is seen to reduce this delay by  $0.08\tau_s$  ( $\sim 0.2\tau_{\alpha\gamma}$ ). These estimations determine the time scales of the delay of  $\gamma$ -emission in TTE (Trace Tritium Experiments) plasmas. In spite of the rather wide energy spectrum of the alpha source and of the essential time spread of the fusion source in the post-blip period the delay of alpha induced  $\gamma$ -emission is well detected, at least in the case of large slowing down times and short blips. This is confirmed by Fig.2 that displays, in 3-dimensional and contour representation, the modelled evolution of  $\alpha$ -induced  $\gamma$ -emission as a function of the alpha energy for a typical tritium NBI blip plasma in JET (Pulse No: 61346,  $\tau_s = 620\text{ms}$ ,  $\tau_{\text{blip}} = 100\text{ms}$ ). As evident there, the maximum  $\gamma$ -ray emissivity is induced by alphas slowed down to energies  $\sim (1.7 \div 2)$  MeV. The peak time of this emission is delayed against the maximum fusion source strength at the end of the T blip by about  $100\text{ms}$ , which is about  $0.15\tau_s$ . As depicted in Fig.3 demonstrating the modelled evolution of gamma emission induced by well confined alphas, the gamma-emission delay increases with longer slowing down times. In Fig.4 we display the modelled delay time of gamma emission, as determined by the time shift of the centroids of  $R_\gamma$  and of the  $\alpha$ -source, as a function of the slowing down time affected by the shape of the energy spectrum of the fusion source. In the case of rapid slowing down ( $\tau_{\alpha\gamma} \approx 0.4\tau_s < 0.1\text{s}$ ) the

delay time  $\tau_d$  coincides with  $\tau_{\alpha\gamma}/2$ , while it is about  $0.6\tau_{\alpha\gamma} \approx 0.24t_s$  in the case of weak slowing down, which corresponds with the delay associated with the  $\delta(t)$ -model source. The occurrence of dissimilar gamma delays for strong and weak slowing down is due to different alpha distribution functions which, for  $E > E_m$ , depend on the ratio  $\tau_{\alpha\gamma}/\tau_{\text{blip}}$ . For instance,  $f_\alpha$  appears quasi-steady-state when this ratio is small, whereas it is essentially non-stationary if  $\tau_{\alpha\gamma}$  is large compared to the blip duration ( $\tau_{\text{blip}} = 0.1\text{s}$ ). Note that  $\tau_d = \tau_{\alpha\gamma}/2$  corresponds to the delay of the modelled step-like shape of  $R_g \sim H(\tau_{\alpha\gamma}-t)$  with  $H(t)$  denoting the Heaviside step function.

The impact of alpha loss on the evolution of alpha induced gamma emission can be evaluated from Eq. (3) as well. For that we show in Fig.5 the calculated delay times of gamma emission as a function of loss time  $\tau_l$  for different slowing-down times and energy spectra of the alpha fusion source. It is seen that strong losses with  $\tau_l < \tau_{\alpha\gamma}$  will drastically reduce the  $\gamma$ -delay time. Moreover, the effect of alpha loss becomes more pronounced if the source energy spectrum is broader. Enhanced slowing down, however, will weaken this spectrum shape effect, as apparent from the dotted curves in Fig.5.

### 3. DELAY OF ALPHA-INDUCED G-EMISSION: EXPERIMENTAL EVIDENCES AND MODELING RESULTS

Our analysis indicates that the most suitable discharges for the observation of gamma delays are those with longer slowing-down times and shorter NBI blip duration. Moreover, such discharges are advantageous for assessing possible alpha loss effects, as only rather strong losses with  $\tau_l < \tau_{\alpha\gamma} \approx 0.4t_s$  are expected to significantly reduce the  $\gamma$ -ray emission delay. Table 1 summarises the basic parameters of 6 short blip TTE discharges with different qualities of alpha confinement, which are subjected to the analysis here. Thus we consider typical TTE Current Hole (CH) plasmas (Pulse No's: 61346, 61347, 61348) and Monotonic Current (MC) plasmas (Pulse No's: 61131, 61151, 61158). The safety factor profiles in MC plasmas are represented in Fig.6 and for CH discharges in Fig.7 correspondingly. It should be pointed out that an evident sawtooth activity was observed during tritium NBI in Pulse No: 61131. Thus Fig.8 demonstrates a nearly 1keV drop of the electron temperature and about 30% reduction of the DT neutron emission in the plasma core, caused by sawtooth activity before the blip end of this shot. Referring to a short blip duration (= 0.1s) and a Spitzer slowing down time in the core of  $\tau_{s0} = 0.69\text{s}$ , Fig.9 displays the time behaviour of the  $\gamma$ -ray intensity  $R_\gamma$  measured in the CH plasma of Pulse no: 61348 ( $I_p/B_t = 2.5\text{MA}/3.2T$ ). The delay of  $\gamma$ -emission becomes apparent from Fig.10 where the measured  $R_\gamma(t)$  is, due to the delay, still higher than the averaged DT neutron emission rate in the considered time interval corresponding to the integration time of the  $\gamma$ -measurements (=250ms). Here the delay time, measured as the shift between the centroids of  $\gamma$ -ray and neutron emission in the time interval of 3×250ms, is 65ms. Figure 11 compares the measured  $R_\gamma(t)$  for CH Pulse No's: 61346 and 61347 with nearly identical plasma parameters ( $I_p/B_t = 2.5\text{MA}/3.2T$ ,  $\tau_{s0} = 0.62-0.64\text{s}$  (see Fig.12)) but with fusion rates different in time. The fact that, contrary to the essential difference of  $R_\gamma(t)$  in both discharges, the delay times are very close ( $t_d \approx 0.08-0.09$ ) illustrates the relevance of  $\tau_d$  as a characteristic of fusion alpha

confinement. Delays of gamma emission in monotonic current plasmas are seen in Fig.13. As expected, a weaker slowing down and degraded alpha confinement will reduce the measured delay times. It is of interest to compare the measured delays with those resulting from a 3D Fokker-Planck model [3, 7] that accounts for first orbit losses only and hence should yield the maximum delay times. Figure 10 demonstrates that the rate of  $\gamma$ -ray emission calculated for CH plasma of Pulse No: 61348 (red curve) overestimates the measured delay time, thus indicating the presence of additional losses of  $\alpha$ -particles or their energy. A significant difference between observed and modelled delay times is found for plasmas with low current (Fig.13(a), (b)) and those with sawtooth activity (Fig.13(c)); in both cases the modeled delays notably exceed the measured  $f_d$ . Figure 14 compares the measured  $\gamma$ -emission delay times with the modelled ones for the JET discharges listed in Table1. As confirmed by Fig.15, we point out that the 3D Fokker-Planck fusion alpha simulation used here is, in view of assessing the delay of alpha induced  $\gamma$ -emission, in good agreement with calculations based on CRONOS/SPOT [6] for Pulse No: 61341.

#### **4. SUMMARY**

Our investigation of the evolution of  $\gamma$ -emission induced by fusion alphas colliding with beryllium impurity ions in tritium NBI blip experiments on JET demonstrates the prospects for using  $\gamma$ -ray diagnostics for studying charged fusion products. Particularly, the possible evaluation of the particle and energy loss rates of fusion alphas via the delay time between alpha induced  $\gamma$ -emission and the fusion source is shown to be a viable technique. Accounting for first orbit loss of alphas only, the 3D Fokker-Planck modelling of gamma emission overestimates the measured delay time thus indicating that additional losses of  $\alpha$ -particles or enhanced energy losses of alphas may exist in this case. A noticeable difference between the observed and the modelled delay times is found in the cases of current hole and low current plasmas as well as in those with sawtooth activity.

Note that modelling of gamma rays produced by energetic ( $E > 5\text{MeV}$ ) minority protons during RF heating in JET [9] also demonstrated the delay of  $\gamma$ -emission calculated in the absence of radial diffusion against the measured one.

In conclusion we note that the relatively low accuracy of the observed delay times in tritium NBI blip experiments on JET was caused mainly by the large integration time of the  $\gamma$ -ray measurements carried out for the first time [1]. For a reliable determination the gamma emission delay, the upper limit of the time resolution of measurements should be around  $0.2\tau_s \sim 0.1\tau_{s0}$  meaning, however, that the alpha source power needs to be increased several times. This can guarantee an acceptable accuracy of alpha confinement evaluation via  $\gamma$ -emission diagnostics in TTE-like plasmas.

#### **ACKNOWLEDGEMENT**

This work has been partially carried out within the Association EURATOM-OEAW and under EFDA.

## REFERENCES

- [1]. V.G. KIPTILY, *et al.*, Phys. Rev. Lett. **93**, 115001 (2004)
- [2]. D. STORK, *et al.*, Nucl. Fusion, **45**, S181 (2005)
- [3]. V. A. YAVORSKIJ, *et al.*, 20<sup>th</sup> IAEA Fusion Energy Conference, Vilamoura, 2004, paper TH/P4-4
- [4]. N. HAWKES, *et al.*, Phys. Rev. Lett. **87**, 115001 (2001)
- [5]. T. FUJITA, *et al.*, Phys. Rev. Lett. **87**, 245001 (2001)
- [6]. M. SCHNEIDER, *et al.*, Phys. Plasmas Contr. Fus. **47**, 2087 (2005)
- [7]. V. A. YAVORSKIJ, *et al.*, 32nd EPS Plasma Physics Conference, Tarragona, Spain, 2005, paper O2/02
- [8]. V.G. KIPTILY, 9th IAEA TM on Energetic Particles, Takayama, Japan, (2005)
- [9]. I. VOITSEKHOVITCH, *et al.*, Nucl. Fusion, to be submitted
- [10]. J.M. ADAMS, *et al.*, Nucl. Fusion, **31**, 891 (1991).

Pulse No:	I/B, MA/T	$\tau_{s0}$ , ms	$q_0$	$\tau_{blip}$ , ms	FO loss, %	$\tau_d^{exp}$ , ms	$\tau_d^{mod}$ , ms
61131	2.3/2	280	<1	150	~19	<26	18
61151	1.4/1.65	420	>1	100	~44.5	3-53	102
61158	2/2.45	440	>1	150	~17	45-106	93
61346	2.5/3.2	620	>>1	100	17-19	40-127	121
61347	2.5/3.2	640	>>1	100	17-19	58-121	135
61348	2.5/3.2	690	>>1	100	18-19	49-128	125

Table 1: Basic parameters and delay times determined for 5×250ms time interval

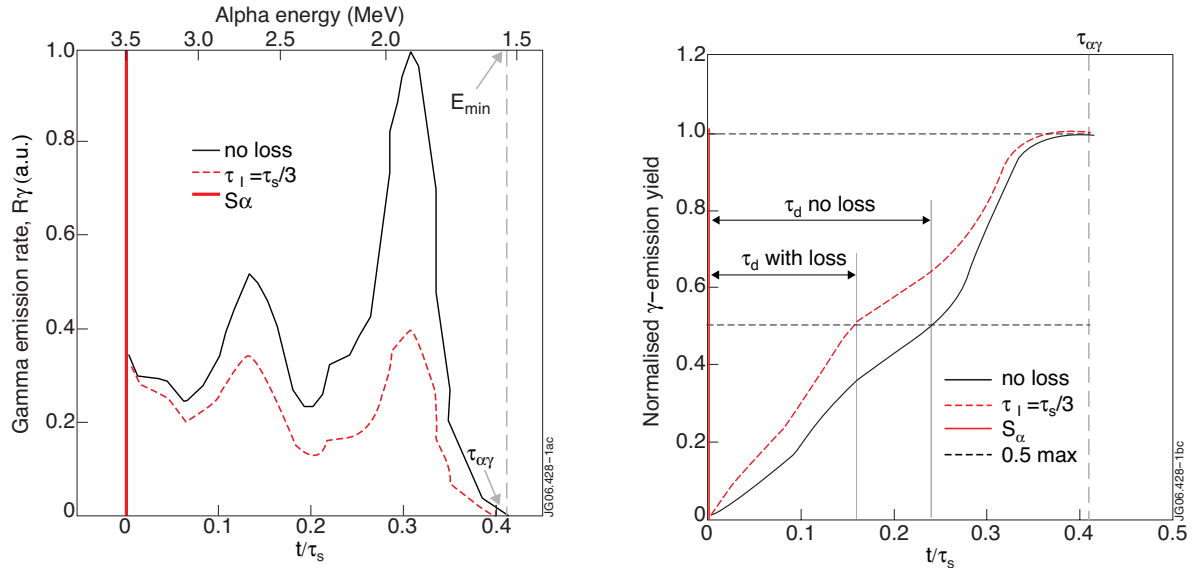


Figure 1: Evolution of gamma emission induced by alphas from a 3.5MeV fusion source effective only at the moment  $t=0$ .

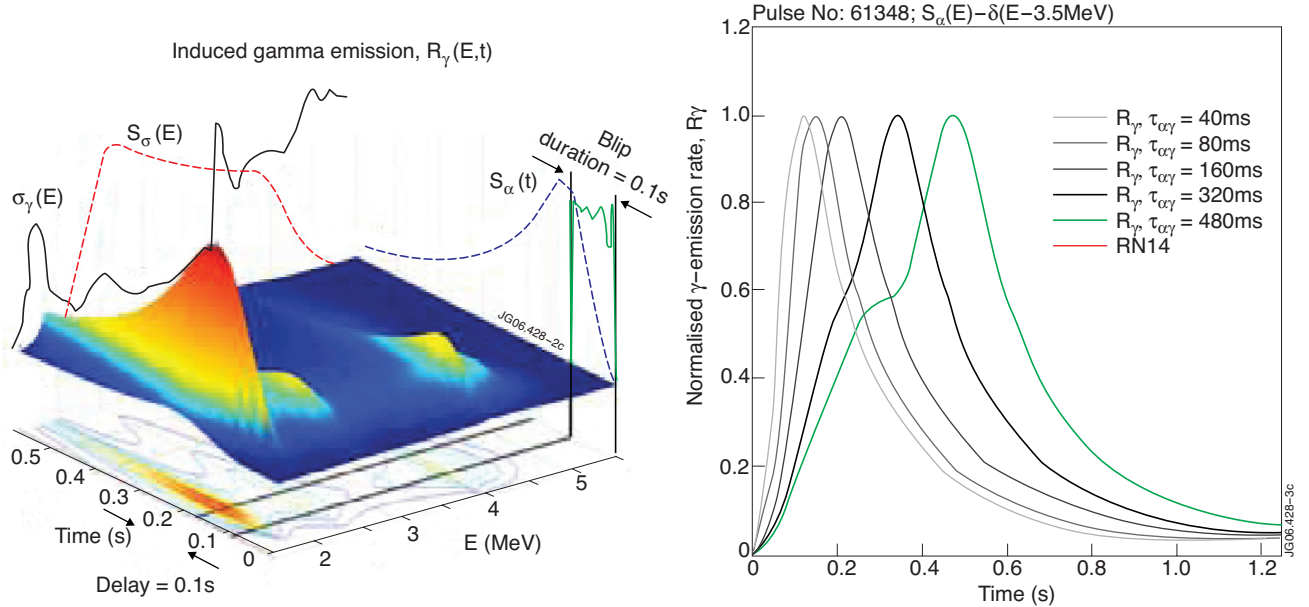


Figure 2: Calculated intensity of alpha induced  $\gamma$ -emission versus time and alpha energy for Pulse No: 61346 (1D Fokker-Planck model,  $\tau_s = 620\text{ms}$ ).

Figure 3: 1D Fokker-Planck evolution of gamma emission induced by well confined alphas from a mono-energetic TTE-like source (Pulse No: 61348) depending on the value of Spitzer slowing-down time in  $\tau^{\alpha\gamma} = 0.5\tau_s \ln(3.5\text{MeV}/E_m)$ .

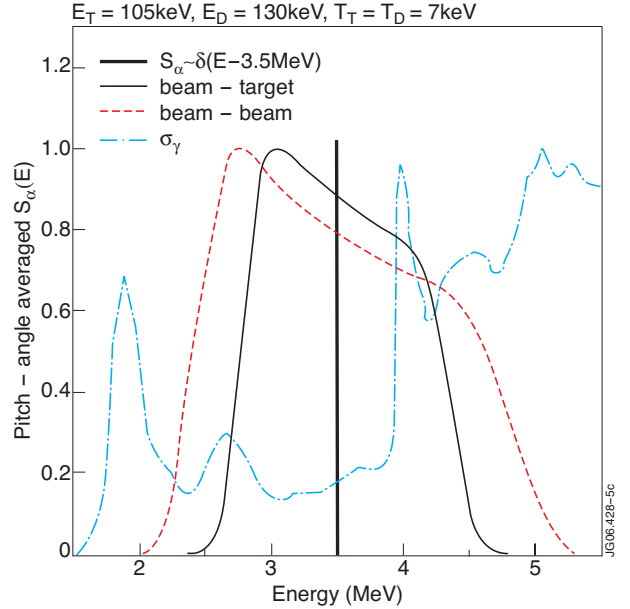
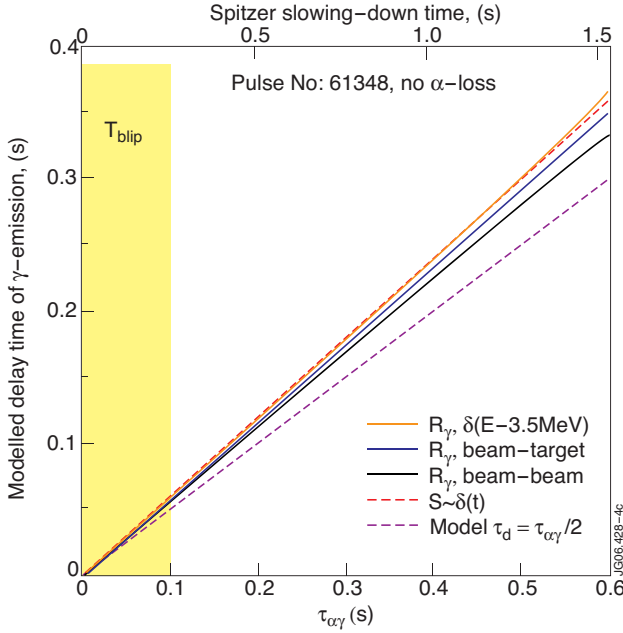


Figure 4: Modelled delay times (left) of gamma emission and of the density of well confined fast alphas ( $E > 1.7\text{MeV}$ ) as a function of slowing-down time for different shapes of the fusion source energy spectrum in Pulse No: 61348 (1D Fokker-Planck model).

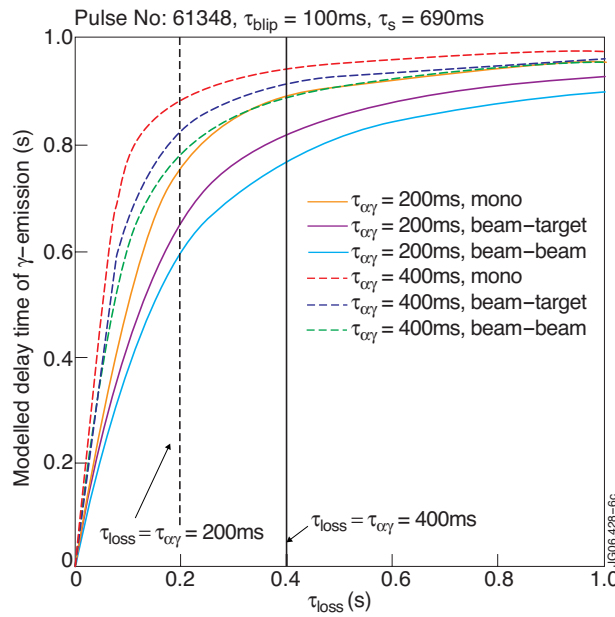


Figure 5: Modelled delay time of gamma emission as a function of average alpha loss time, displayed for two slowing-down times  $\tau_{\alpha\gamma} = 400\text{ms}$  and  $200\text{ms}$ , and for different energy spectra of the fusion source in JET Pulse No: 61348.

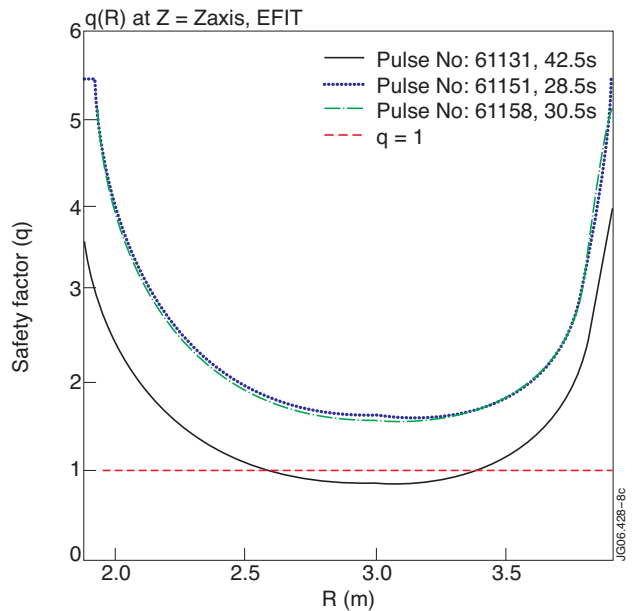


Figure 6: EFIT mid-plane  $q$  profiles at the beginning of  $T$  blimp for MC Pulse No's: 61131, 61151 and 61158.

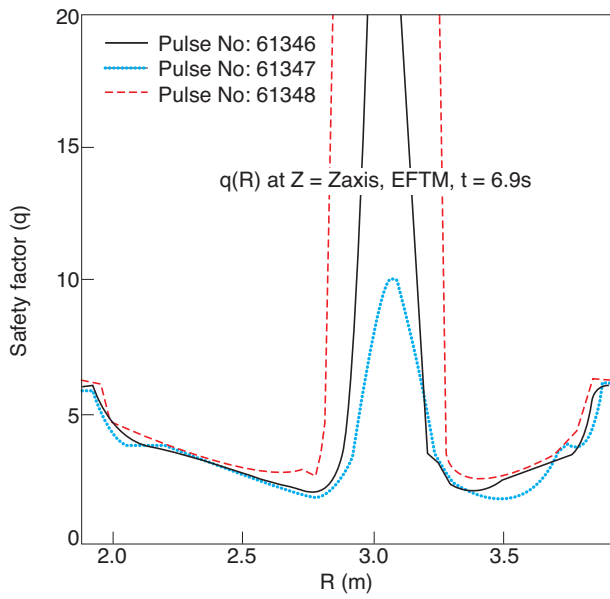


Figure 7: EFTM mid-plane  $q$  profiles in early post-blip CH Pulse No's: 61346, 61347 and 61348 (<0.3s after the end of blip).

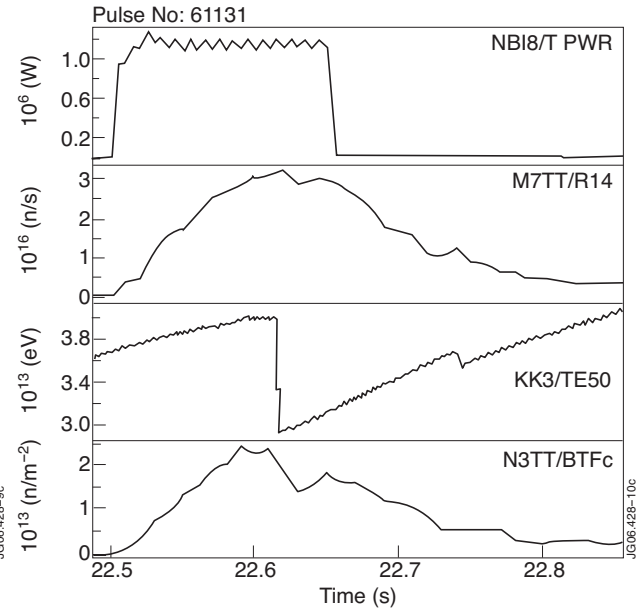


Figure 8: Sawtooth effect on electron temperature and DT fusion neutron emissivity during tritium blip in TTE shot Pulse No: 61131.

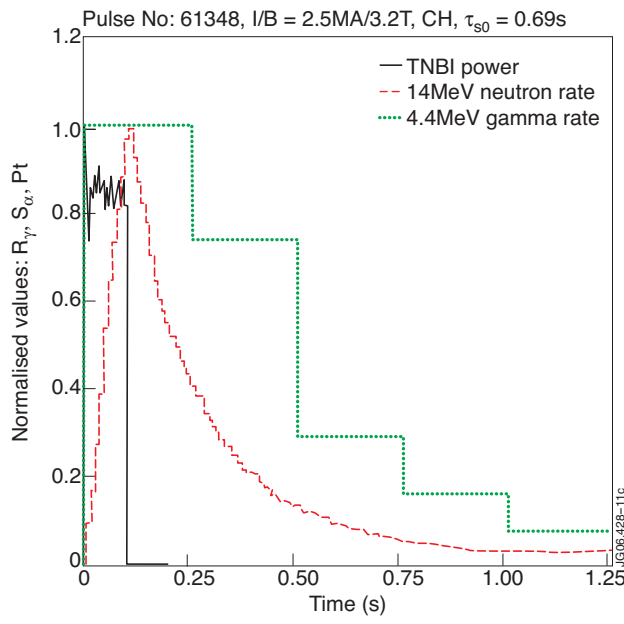


Figure 9: Measured rates of gamma and neutron emission for JET Pulse No: 61348. The orange curve represents the tritium NBI power.

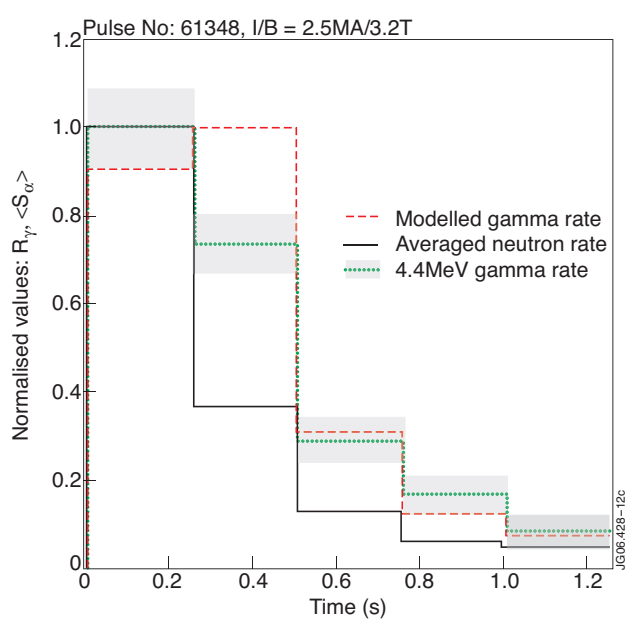


Figure 10: Measured rates of gamma and neutron emission (averaged over 250ms integration times of  $g$ -measurements) and modelled  $R_g$  for JET Pulse No: 61348.

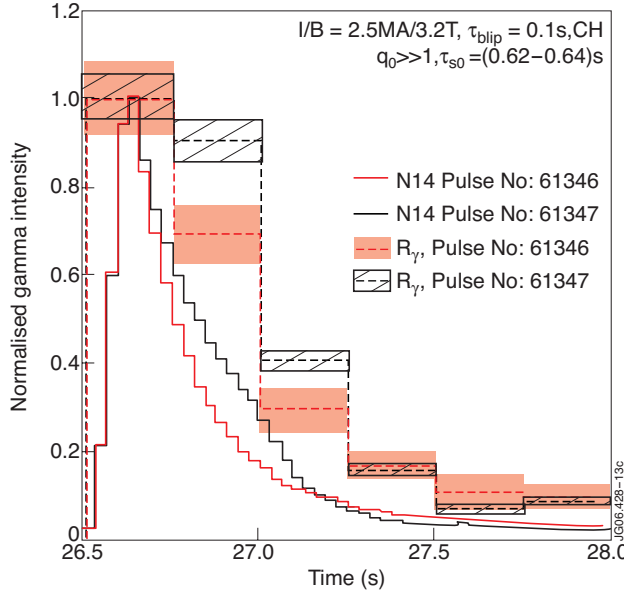


Figure 11: Measured gamma rates for Pulse No's: 61346 and 61347.  $\tau_d \approx 0.08\text{--}0.09\text{s}$  is weakly dependent on the fusion source's time dependence.

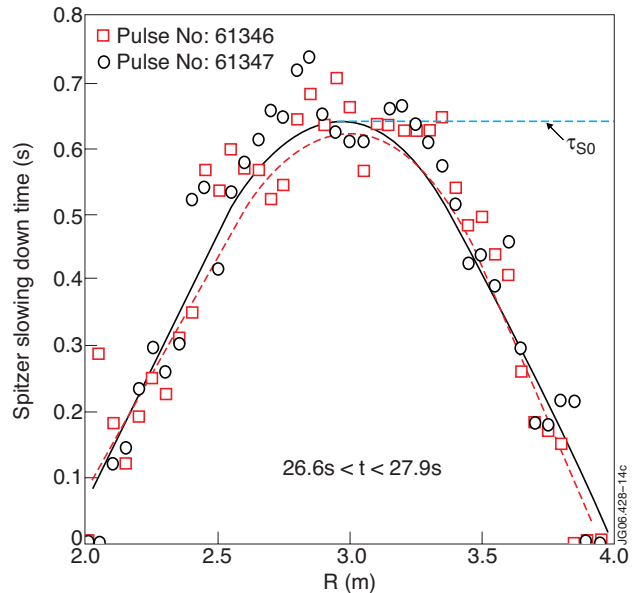


Figure 12: Time averaged mid-plane profiles of Spitzer times of alphas for Pulse No's: 61346 ( $\tau_{s0}=0.62\text{s}$ ) and 61347 ( $\tau_{s0}=0.64\text{s}$ ).

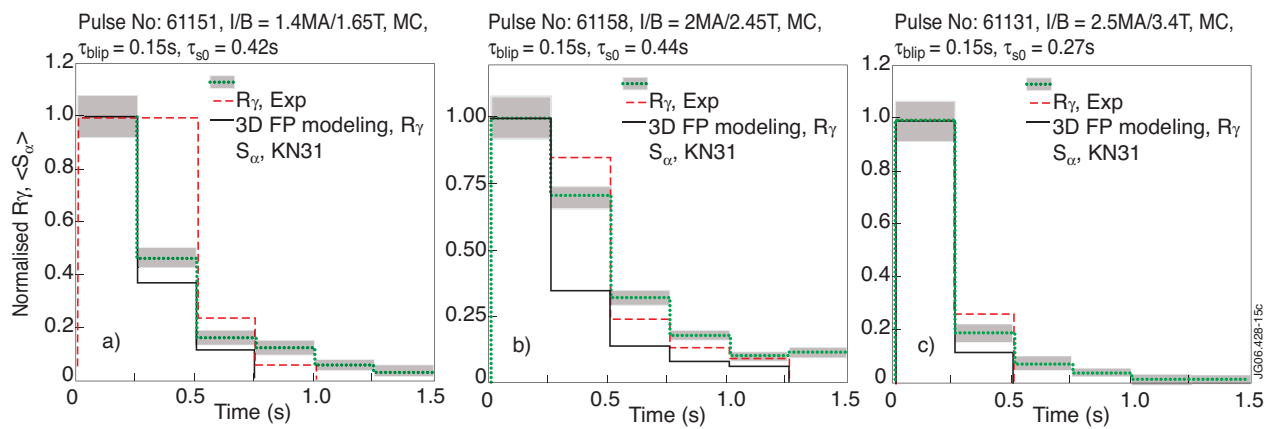


Figure 13: Measured and modelled rates of gamma and neutron emission in the cases of plasmas with low current (figure a, b) and in those with sawtooth activity (figure c ).

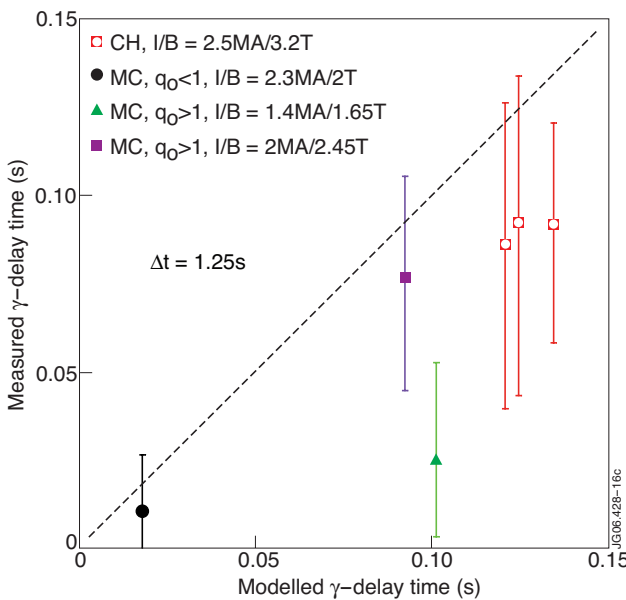


Figure 14: Measured versus modelled delay times of  $\gamma$ -emission based on 3D FP modelling for CH (Pulse No's: 61346 ÷ 61348) and MC (Pulse No's: 61131, 61151, 61158) plasmas in JET.

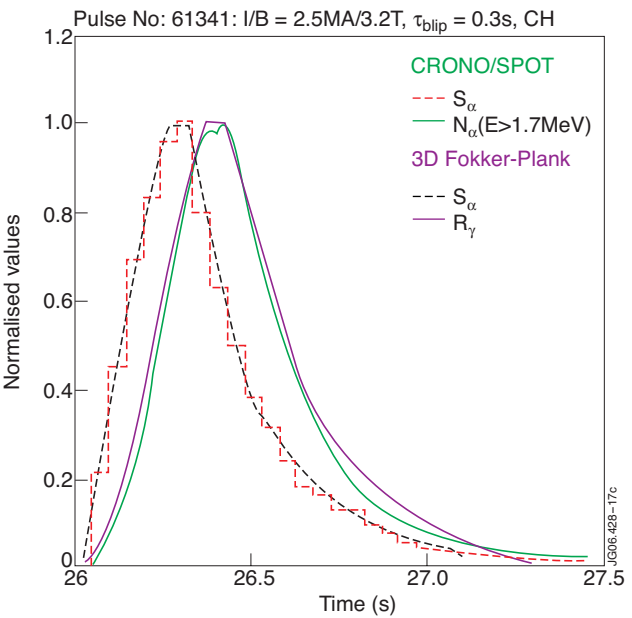


Figure 15: Comparison of Fokker-Planck modelled  $\gamma$ -emission rate,  $R_\gamma$  (violet curve) and CRONOS/SPOT calculations of  $N_\alpha(E > 1.7\text{MeV})$  (green curve) for Pulse No: 61341.